JAST, Vol. 10, No. 2, pp. 1- 7

JAST
Journal of Aerospace Science and Technology

(Research Note)

Experimental Investigation ofthe Hovering Performance of aTwin-Rotor Test Model

F. Shahmiri[1]

1. Department of Aerospace Engineering, MalekAshter University of Technology

*Postal Code: 158751774, Tehran, IRAN

prof.shahmiri@gmail.com

Hover performance of a twin-rotor test model in terms of rotor overlap sweep, blade collective pitch, and blade tip speedwasexaminedexperimentally.The experimental setup consisted of two three-bladed rotors (tandem rotor configuration) with a diameter of1,220 mm and constant chord of 38 mm, giving a blade aspect ratio of 16.05. The blades were of a rectangular planform with NACA 0012 cross-sections with no twist or taper. In this model, the front rotor was fixed on the fuselage and the rearrotor could move longitudinally for tests up to about40% rotor overlap sweep.To accurately examine the hover performance, thrust, power required, power loading (PL), and figure of merit (FM) responses were measured usinga central compositetest plan. Furthermore, four quadratic polynomialswere fitted to all responses, necessary for a better understanding of the main effects and interactions. The results clearlyshowed that significant interactions between variables are evident and therefore overlapping at constant collective pitch reduces thrust much more than reducingthe power required. Moreover, the results showed that, for the twin-rotor system,the maximumefficiency in hover (i.e., maximum power loadingof 14.6kg/kW) is obtainedfor no overlapped rotors at low values of disc loading and blade tip speed.Experimental measurements of thetwin-rotor hover performance based on a central composite plan andinteraction analysis were the main contributionsstated in the current work.Results for the twin-rotor test model can be generalized to actual tandem helicopters through the Reynolds number transformation technique and some modifications.

Keywords: Twin-rotor; Rotor overlap sweep; Central composite design; Wind tunnel test; Hoveringperformance

Introduction

Generally, the tandem rotor systems offer design advantages over conventional single rotor configurations. Additional power requirements and weight associated with the tail rotor, tail boom, and transmission system may be assigned for additional useful loads in tandem rotor configurations. Furthermore, the asymmetry of lift associated with a single rotor system in forward flight is reduced, andtherefore itoffers great potential fora faster and more stable vehicle. Reductions in the power required at hover and low forward flight speed are also advantages cited for tandem rotor configurations [1-2].

However, in a tandem rotor configuration, aportionof front rotor continually operates in the flow of rear rotor. In this common portion (rotor-overlap), flows of rotors interact with each other and produce a more complicated flow field than a single rotor configuration. This overlapped area causes a loss of net aerodynamic efficiency and it results in significant effects on flight performance that is attributed to the increase of both induced and profile power (viscous) losses.

Blade element momentum theory (BEMT)successfully showed a simple representation of hover performance for tandem rotors [3,4]. Using BEMT, onlya qualitative prediction of global behavior of performance with simplified assumptions was obvious. For example, Harris approximateda power expression for tandem rotor helicopters with theideal twist assumption while the profile power was assumed to be minimum [3,5]. However, because of the assumptions used, this formulation was confined to a particular blade loading for twin-rotor systems.

1. Assistant Professor
Tel: +98 (21) 88726851

The vortex theory is also used for calculating the flowfield of rotor wake in single main rotors. Unlike BEMT, a higher-level approximation of the fluid flow equations coupled with a representation of the blade geometry was achieved [6,7]. This representation of the performances wasmore realisticthanBEMTbecause of the consideration of local flow characteristics. However, the result of vortex theory for twin-rotor configurations comes at a significantly larger cost and it is used only for thedevelopment of rotor aerodynamic concepts. Vortex methodrequires an enormous computational cost needed to handle the counter-rotating system. Furthermore, to capture the blade–vortex and vortex–vortex interactions correctly, it is important to accurately represent the formation and evolution of the wake. Therefore, accurate numerical schemes, extremely high resolution meshes, and reliable turbulence models must be employed, and the results must be carefully validated with reliable experiments.

The first tests on twin-rotor helicopters were performed byStepniewski, resulting in a rotor overlap correction factor for the required power [6,7]. This factor is used for increasing the power and thrust first, and then for the induced power only when two rotors overlap at a constant thrust [8-10]. Following this, Halliday and Cox also conducteda series of tests on a particular twin-rotor model to extensively study twin-rotor performance in hover and forward flight [11].

All tests for examining hoverperformance mentioned above share a common problem in that the data have not been published, and they are, therefore, limited to main effect studies without attention to interaction analyses. Significant interactions between rotor variablesareinvolvedin hover efficiency for twin-rotor configurations, and so many hypotheses can be tested. Accordingly, the sufficient test data and quadratic models are desirable in the study of twin-rotorhovering performance. For rapid restatement of the effects of the main variables and their interactions in hover performance, firstbefore doing experiments, a test planwasdesignedusing central composite design (CCD) [12,13], and then the quadratic polynomials of thrust coefficient, power required, power loading (PL), and figure of merit (FM) were developed in the present paper.Therefore, the effects of rotor overlap sweep, blade tip speed, and blade collective pitch on hover trends as well as optimal conditions for maximum hover aerodynamic efficiency were determined.

Experimental setup

All the experiments were conducted on a small-scale twin-rotor model, as illustrated in Fig.1. This model had two three-bladed rotors with the same diameter of 1,220 mm, mounted on a sliding rail that was appropriate for the ease of longitudinal movements of the rear rotor relative to the fixed front rotor. Using this rail, the various combinations of rotor overlap sweeps (ratio of hub separation distance, d, to rotor diameter, D.) suggestedby CCD wasachieved (see Fig. 1). In this model, the rotor blades had a rectangular planform with NACA 0012 cross-sections made of composite carbon fiber and had no twist or taper. Therefore, each blade had a constant chord length of 38 mm and aspect ratio of 16.05, as summarized in Table 1. Furthermore, no flap and nolead-lag hinges were incorporated into the blade root attachments, because the rotor hubs were designed and built on the basis of thehinge less rotor considerations, andthus no physical hinge offset was incorporated into the test model.

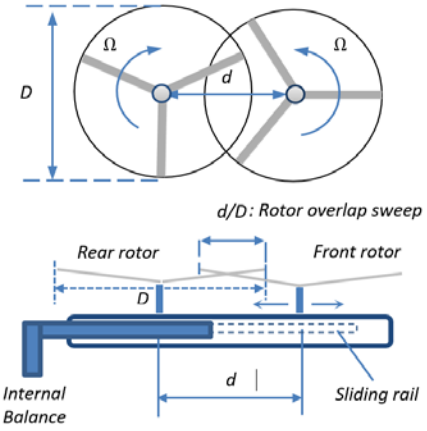

Figure 1. Twin-rotor model configuration.

Table 1. Specifications of the twin-rotor test model.

Variables	Values
Number of main rotor	2
Rotor diameter=D1=D_2=2R	1,220 mm
Blade chord length, c	38 mm
Number of blades	3
Blade twist, θtw	0 deg.
Blade taper, ct/cr	none
Aspect ratio, AR=R/c	16.05
Rotor solidity, Nc/πR	0.056
Blade tip speed, vtip=RΩ	100-120 m/s
Airfoil section	NACA 0012
Rotor rotational speed, RPM	1,600-1,800 RPM
Tip Reynolds number	270,000-340,000

The sliding railwasfinally installed on a stand with a six-component internal balance that was able to measure the forces and moments in 2.2×2.8 subsonic wind tunnel, as illustrated in Fig. 2. This tunnel was a type of close-circuit and low speed tunnel that was used for testing different models. A great feature of the tunnel was the capacity to work as an open test section outline by removing the walls. Consequently, the test swereper formed in the open test section that allowed maximum access and had no ground effects.

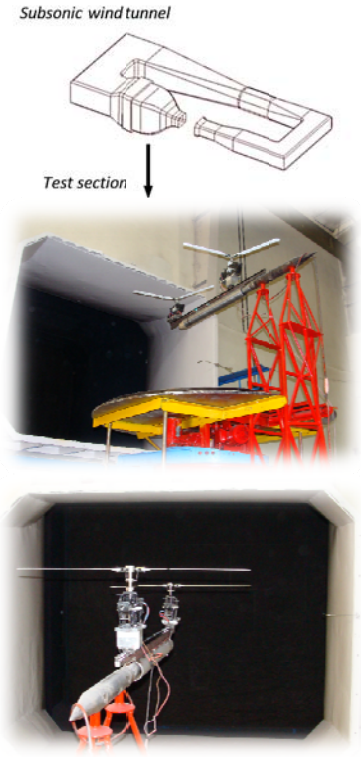

Figure 2. Subsonic wind tunnel and test model.

Tests and data measurements

In the present research, 20 pointswere designed for three variables named blade collective pitch (θ_0), blade tip speed (v_{tip}), and rotor overlap sweep (d/D). Using CCD structure, the total number of experiments were limited to2^k+2k+6 (=20) for k=3. These points were2^k factorial, 2k axial, and 6 arbitrary central points, necessary for pure error estimation of experiments. Figure 3 shows the distribution of the points through the design space. As seen, the factorial points are at the corners and the axial points were located at the distance of $2^{k/4}$ from the 6 central points (0,0,0). Due to simplicity, the coordinate of points was changed into the coded or non-dimensional values, and so the five levels including -1.68, -1, 0, +1, and +1.68, were assessed by the whole 20 points. With these five levels any curvature of response and interactions between variables could be achieved by quadratic polynomials fitted to measurements.

The measurementswere made for thrust coefficient (C_T), power coefficient (C_P), power loading (PL=T/P), and figure of merit (FM)response at hover condition (Table 2). The selection of responses was a challenge of the present work, but the trade-off studies showed that C_T, C_P, PL, and FM can be used for the twin-rotor hover aerodynamic efficiency representation. Therefore, the thrust and power coefficients were redefined as [14]:

The experiments were designed for three candidate variables (i.e., rotor overlap sweep, d/D, blade tip speed, v_{tip}, and blade collective pitch, θ_0) using CCD method. Because the number of variables was set to three, the total number of runs was 20. As shown in Fig.3, these runs included 8 factorials, 6 axials, and 6 replicated center points that were necessary for estimating of experimental errors. Of the different experiments conducted, Table 2 shows the cases that were chosen for measuring thrust coefficient(C_T), power coefficient (C_P), power loading (PL=T/P), and figure of merit (FM)for the twin-rotor model, respectively. Therefore, using these four responses, the aerodynamic efficiency of the twin-rotor model in hover could be gained and discussed. Note that the thrust and power coefficients were defined as;[14]

$$C_T = \frac{T}{\rho A v_{tip}^2} \; C_P = \frac{P}{\rho A v_{tip}^3} \tag{1}$$

Also, the power loading (i.e., thrust to total power ratio) and figure of merit (i.e., induced power to total power ratio) were defined through BEMT as;[14]

$$PL = \frac{T}{P} = \frac{C_T}{v_{tip} C_P}$$
$$FM = \frac{T}{P}\sqrt{\frac{T}{A}}\left(\frac{1}{\sqrt{2\rho}}\right) = \frac{PL\sqrt{DL}}{\sqrt{2\rho}} \tag{2}$$

where ρ is air density, A is $2\pi R^2$, $v_{tip}$is RΩ, and T/A denotesthedisc loading (DL).

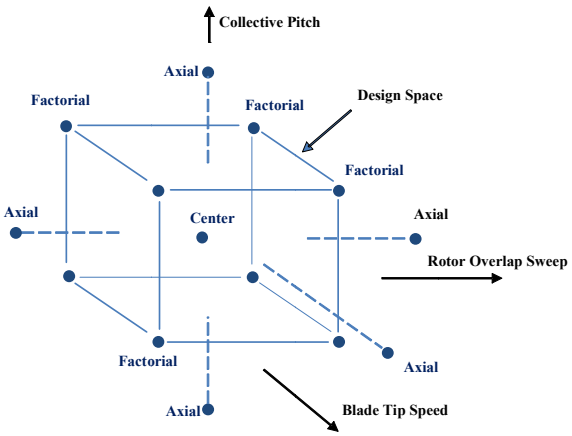

Figure 3. Schematic of CCDspace with three variables (i.e., rotor overlap sweep, blade tip speed, and collective pitch).

Table 2. Test conditions and measured responses for the twin-rotor in hover.

Run	Variables				Responses			
	d/D	v_{tip} (m/s)	θ_0 (deg.)		C_T	C_P	PL (kg/kW)	FM
1	0.7	106	10.6		0.0051	0.0004	11.9	0.67
2	0.6	115	9.3		0.0043	0.0003	10.9	0.63
3	1	106	10.6		0.0053	0.0004	12.2	0.7
4	1	115	9.3		0.0046	0.0003	11.4	0.68
5	0.8	130	9.3		0.0044	0.0003	8.7	0.58
6	0.7	124	7.9		0.0036	0.0003	10.1	0.56
7	0.8	115	9.3		0.0044	0.0003	11.2	0.67
8	1	106	7.9		0.0037	0.0003	13.4	0.64

Run	Variables				Responses			
9	0.7	106	7.9		0.0035	0.0003	12.9	0.61
10	0.8	100	9.3		0.0044	0.0003	13.6	0.66
11	0.8	115	9.3		0.0044	0.0003	11.2	0.67
12	1	124	10.6		0.0053	0.0004	9.2	0.66
13	1	124	7.9		0.0037	0.0003	10.4	0.59
14	0.8	115	9.3		0.0044	0.0003	11.2	0.67
15	0.8	115	9.3		0.0044	0.0003	11.2	0.67
16	0.8	115	11.5		0.0058	0.0005	10.2	0.69
17	0.8	115	9.3		0.0044	0.0003	11.2	0.67
18	0.8	115	7		0.0031	0.0002	12.1	0.58
19	0.7	124	10.6		0.0051	0.0004	9.1	0.63
20	0.8	115	9.3		0.0044	0.0003	11.2	0.67

Results and discussion

The quadratic modelsamongseveral modelswere chosen in the present study. Thus, fourmodels were fittedto all measured responses given in Table 2. Thesequadratic models that were found to be adequate for the prediction of hoverperformance are given by:

$$10^3 C_T = 4.39 + 0.17A + 0.06B + 1.29C + 0.03AC - 0.07A^2 + 0.09B^2 \quad (3)$$

$$10^5 C_P = 32.8 + 0.5A + 3.9B + 11.9C + 3.7B^2 + 1.5C^2 \quad (4)$$

$$FM = 0.63 + 0.026A - 0.06B + 0.056C - 0.01A^2 - 0.05B^2 - 0.03C^2 \quad (5)$$

$$PL = 11.6 + 0.26A - 3.8B - 0.71C + 0.2\,BC - 0.14A^2 - 1.6B^2 - 0.36C^2 \quad (6)$$

where all the variables are no dimensional and A is rotor overlap sweep, B is blade tip speed, and C is collective pitch. In addition, AB, AC, and BC are interaction of main variables. Figs. 4 and 5 show thepredicted againstmeasured valuesof thrust and power coefficients, respectively. Also, values of R-square (R^2), which is the area measurementof the variations around the mean values of the models, were shown in the figures.[13] The high value of R-square showed that the quadratic models, Eqs. (3)-(4), are capable of representing the system under the given experimental domain (see Figs. 4 and 5).

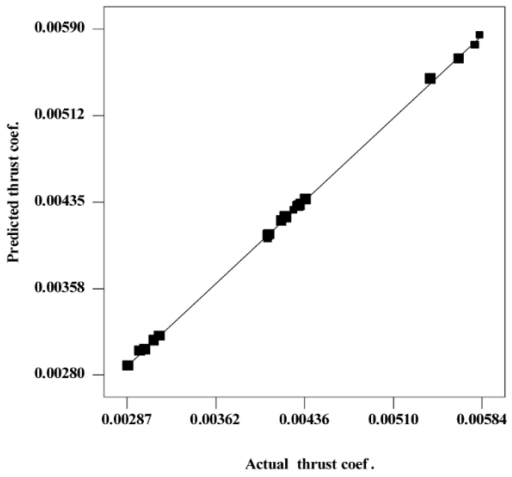

Figure 4. Comparison of measured and calculated thrust coefficients for the twin-rotor in hover (R2=0.9997).

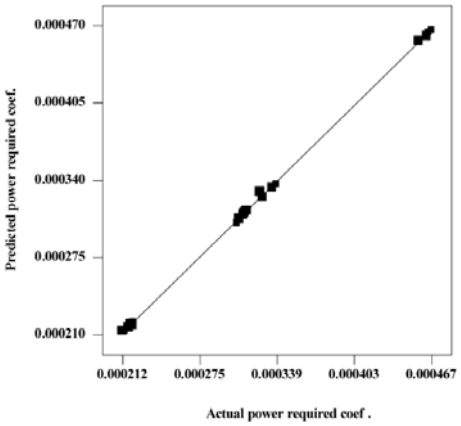

Figure 5. Comparison of measured and calculated power coefficientsfor the twin-rotor in hover (R^2=0.9995)

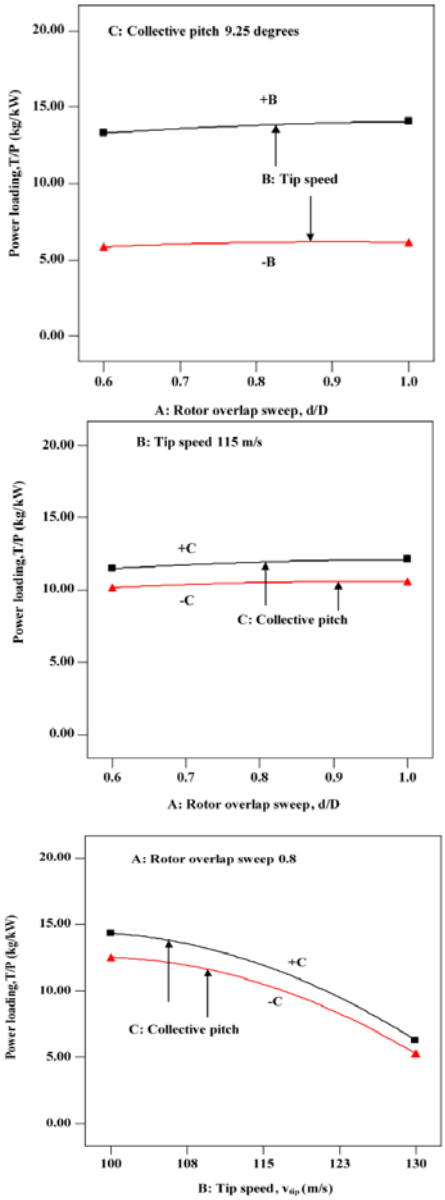

Figure 6. Effects of interaction between variables on PL response. (a): Effects of AB interaction; (b): Effects of AC interaction; (c): Effects of BC interaction

However, the interactions between variables hadsignificant effects on the responses. Therefore, the predicted responses were presented and discussed in terms of interactions as well. Fig. 6(a), 6(b), and 6(c) show the effects of interaction terms (i.e., AB, AC, and BC) on the PL response. In these figures, the red and black lines denote the lowest (-1) and the highest level (+1) for the variable of interest, respectively.

Unlike the parallel lines in Figs. 6(a) and 6(b), the non-parallel lines in Fig. 6(c) confirms significant interaction between B and C. This means that the effect of blade tip speed on power loading response is different at different values of the collective pitch.

Figs. 7 and 8 showthe effects of rotor overlap sweep (A), blade tip speed (B), and collective pitch (C) on the figure of merit and power loading responses. To better understand the effects of each variable, a reference pointwaschosen at (0,0,0), corresponding tod/D=0.8, v_{tip}=115 m/s, and collective pitch of 9.25degrees. As seen,figure of meritdependsmore on the collective pitch rather than the rotor overlap sweep and the blade tip speed.Furthermore, the collective pitchhas shown a positive effect onfigure of merit, and hence it has been the most significant variable affectingfigure of merit in comparison with the other twovariables.However, Fig.8exhibits that the power loading depends more on the tip speed values, a result that isin agreement with BEMT, where the tip speed appeared in the denominator of power loading expression (see Eq. (2)).

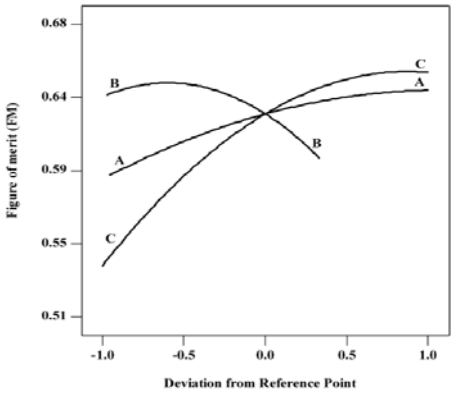

Figure 7. Effectsof rotor overlap sweep, blade tip speed, and collective pitch on figure of merit at d/D=0.8, v_{tip}=115 m/s, and collective pitch of 9.25 degrees.

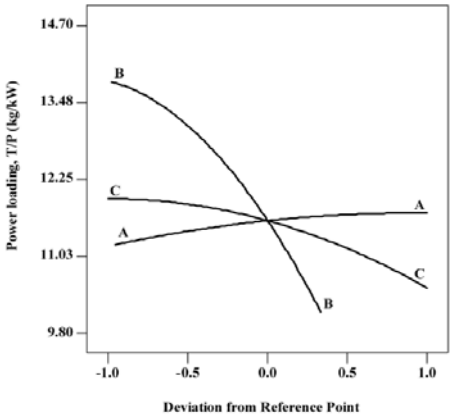

Figure 8. Effects of rotor overlap sweep, blade tip speed, and collective pitch on power loading at d/D=0.8, v_{tip}=115 m/s, and collective pitch of 9.25 degrees.

Fig.9 shows the measured power loading with respect to disc loading for various combinations of candidate variables. The data points include measurements at overlap sweep of 0.6, 0.8, 0.9, and 1.0, tip speed of 100 and 115 m/s, and for the blade collective pitch of 7, 9, and 11.5degrees.

The maximum power loading at the lowest value of disc loadingis evident in Fig. 9. Therefore, in this case, due to the lowest value of induced power loss, the best aerodynamic efficiency in hover for the twin-rotor is obtained. However, in this condition, the figure of merit is nearly closed to 0.6 and significantly less than the ideal figure of merit (FM=1). This result is expected, because the ideal figure of merit was obtained by momentum theory based on the ideal flow assumption (no profile loss). From Fig.9, overlapping at constant collective pitch and blade tip speed reduces the disc loading slightly, and then lower aerodynamic efficiency for the twin-rotor is gained. It has to be mentioned that because figure of merit was dependent on both the disc loading and the power loading, only power loading was chosen as an absolute metric for hover aerodynamic efficiency, and so the best efficiency was addressed by the maximum power loading. Accordingly, its maximum valueat the blade tip speed of 100 m/s and collective pitch of 7 degrees for the non-overlapped (i.e., isolated rotors) system was achieved.

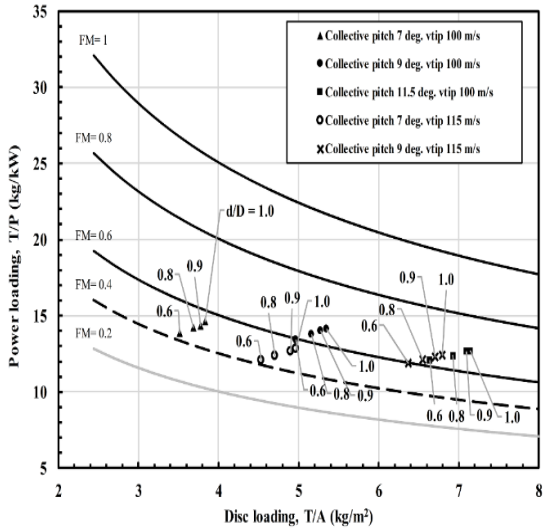

Figure 9. Power loading versus disc loading at different overlap sweeps

Fig.10 shows the measured hover performance with increasing overlap at constant collective pitch and blade tip speed. Also, approximate fairings for data at d/D=1 and d/D=0.6 is shown in the figure.Obviously, the figure shows overlapping at constant collective pitch reduces thrust much more than it reduces power. Typically, the C_T improves by about 8%, and also 3% improvement for the required powerspossible. Theresults also show that increasingthe tip speed at constant collective pitch increases power by about 7%, a result that can be attributed to constant thrust and high profile power loss effects.

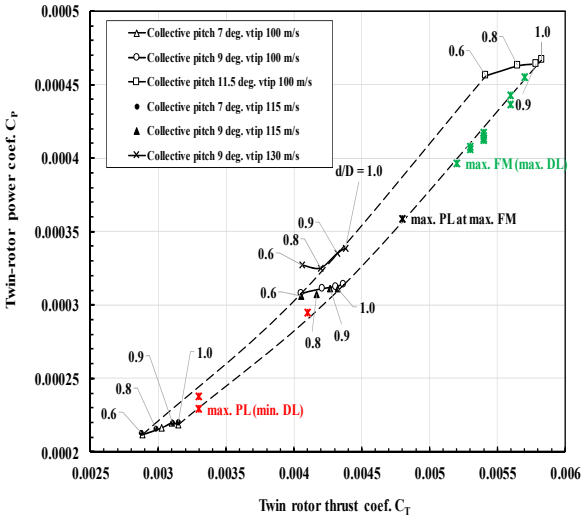

Figure 10. Power required versus thrust in hover

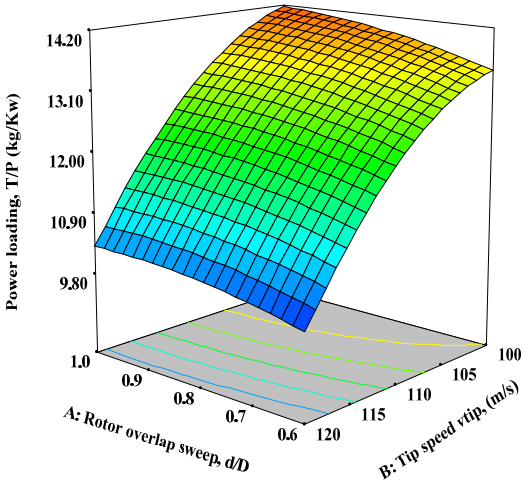

(b)

Figure 11. Comparison of the maximum power loading (kg/kW) and figure of merit of twin-rotor in hover in a range of variables. (a): contour plot; (b): 3D plot.

Fig.11 compares the optimal conditions for three variables when the power loading and figure of merit simultaneously approached to maximum values. A large difference between optimum values in each case isseen. This result is expected, because the maximum figure of merit was attained at higher disc loading, whereas test results showed that the power loading is approximately proportional to $1/\sqrt{DL}$.

Fig.12 compares the measured and calculated power coefficient that was derived for an equal solidity twin-rotor system with ideal blade twist distribution. It is apparent that, for all cases, the difference between experiments and BEMT is less than 5%. A maximum difference at blade tip speed of 130 m/s and collective pitch of 12 degrees is seen; a result that can be referred to minimum profile power proposed by BEMT.

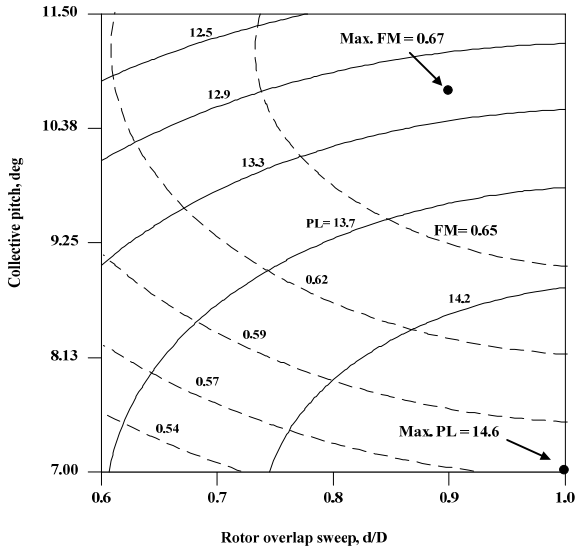

(a)

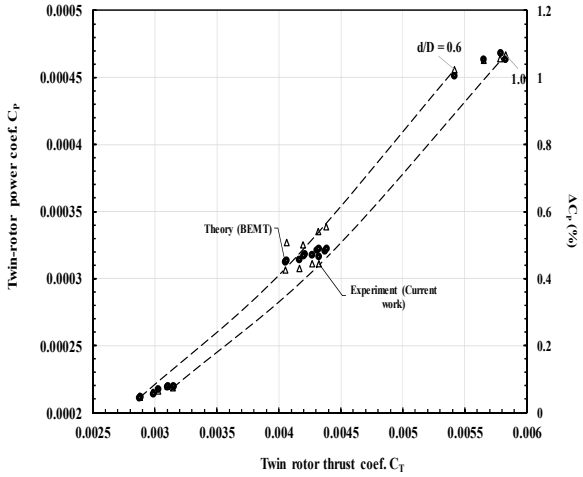

Figure 12. Comparison of the measured and calculated C_P for different overlap sweeps.

Conclusions

Thrust and required power as well as power loading and figure of merit in hovering flight was measured for a twin-rotor test model in a wind tunnel. The experimental set up consisted of two three-bladed rotors with the same diameter of 1,220mm. The blades were of a rectangular planform, were untwisted and with no taper. The aspect ratio of the blade was 16.05. The blade used a NACA 0012 airfoil section along the entire span. A pre-cone angle of zero were set for the blades. Of the different experiments performed based on CCD test plan, Table 2 showed the cases that were chosen for discussion about thrust, required power, power loading, and figure of merit in the present work. The following are the specific conclusions noted in this study:

1. The use of CCD test plan was seen to be essential to lower the costs and to predict the performance of twin-rotor configurations.
2. The best aerodynamic efficiency (maximum power loading) in hover was obtained for no overlapped rotors at low values of disc loading. In this case, maximum figure of merit was about 0.6.

   Overlapping at constant collective pitch reduced thrust much more than reducing the power. Typically, the C_T improved by about 8%, and 3% improvement for power .
3. required was possible. Increasing tip speed at constant collective pitch increased power by about 7%, a result that was attributed to constant thrust and high profile power loss effects.

Acknowledgements

The author thanks the staff in wind tunnel test laboratory of Aviation Industrial Corporation who made contributions to this paper.

References

1. Schrage, D. Design Concepts for an Advanced Cargo Rotorcraft. *JAHS,* Vol. 34, No. 4, 1989, pp. 55-65.
2. Coleman, C. A Survey of Theoretical and Experimental Coaxial Rotor Aerodynamic Research. Moffet Field, 1997, NASA Technical Paper, 3675.
3. Harris, D., Twin Rotor Hover Performance. *JAHS,* Vol. 44, No. 1, 1999, pp. 34-37.
4. Bagai, A., Leishman, G., "Free Wake Analysis of Tandem, Tilt Rotor and Coaxial Rotor Configurations," *JAHS,* Vol. **41, No.** 3, 1996, pp. 196-207.
5. Harris, D., Introduction to Autogyros, Helicopter, and Other V/STOL Aircraft (Vol. 2)., Piedmont, Oklahoma: Ames Research Center Moffett Field, California, 2012, pp. 94035-1000.
6. Rutkowski, M., Gene, R., Ormiston, R., Saberi, H., "Comprehensive Aeromechanics Analysis of Complex Rotorcraft Using 2GCHAS," *JAHS,*Vol. 40, No. 4, 1995, pp. 3-17.
7. Lim, J., Anastassiades, T., "Correlation of 2GCHAS Analysis with Experimental Data," *JAHS,* Vol. 40, No. 4, 1995 pp. 18-33.
8. Halliday, S., Cox, D. *Wind Tunnel Experiments on a Model of a Tandem Rotor Helicopter*, 1961, London: Ministry of Aviation, Aeronautical Research Council.
9. Stepniewski, W.Z., Sloan, L.H., Experimental Investigation of PV-14 Overlap Part I-Downwash Distribution. 1948, Piasecki Helicopter Corp.
10. Stepniewski, W. Z. A., Simplified Approach to the Aerodynamic Rotor Interference of Tandem Helicopters, West Coast American Helicopter society Meeting, 1955.
11. Stepneiwski, W. Z. Rotary-Wing Aerodynamics: Basic Theories of Rotor Aerodynamics (with Application to Helicopters) (Vol. I). 1979, New York: Dover Pub.
12. Mongomery, D. C., *Design and Analysis of Experiments*, New York: John Wiley and Sons, 2001.
13. Myers, H., Montgomery, C., *Response Surface Methodology,* John Wiley and Sons, New York, *2002*.
14. Leishman, J. G., *Principles of Helicopter Aerodynamics* (2^{nd}.), United State of America, England: Cambridge University Press, 2001.